

# Measurement of OZI rule violation and spin alignment in $\phi$ and $\omega$ production at COMPASS

Johannes Bernhard<sup>a</sup> on behalf of the COMPASS Collaboration

Institut für Kernphysik, Johannes-Gutenberg-Universität,  
Johann-Joachim-Becher-Weg 45, 55099 Mainz, Germany

**Abstract.** The COMPASS collaboration at CERN dedicated the 2008 and 2009 run time to hadron spectroscopy measurements with emphasis on the mesonic sector. At 190 GeV/c beam momentum, diffractive and double-Reggeon/Pomeron production mechanisms contribute. Studying vector meson production allows to explore this relatively unknown transition domain. We present results on the ratio of production yields for  $pp \rightarrow pp\phi(1020)$  and  $pp \rightarrow pp\omega(782)$  and its  $x_F$  dependence where we find an OZI rule violation in the order of a factor of 3. In addition, the spin alignment of  $\omega$  and  $\phi$  as a function of  $x_F$  is investigated.

## 1 Introduction

The interplay of production mechanisms such as diffractive, central or Coulomb production at medium beam energies in the order of 100 GeV has been poorly investigated. One approach to single out the different mechanisms is a study of the production of well-known vector mesons, *e.g.*  $\phi(1020)$  and  $\omega(782)$ , exploring the Okubo-Zweig-Iizuka (OZI) rule [1] which states that only processes with connected quark lines are allowed. Due to the deviation from ideal mixing of the  $\phi$  and  $\omega$  mesons, the production cross section ratio  $R(\phi/\omega)$  is determined within the OZI model to be  $4.2 \cdot 10^{-3}$  in any reaction with non-strange hadrons [2]. This has been found to be well-fulfilled in a multitude of reactions [3] at several beam energies [4], but apparent violations were observed in proton - anti-proton annihilations at rest and in nucleon-nucleon collisions. The effect has been interpreted by a polarised strangeness component in the nucleon [5] or a flavour-democratic behaviour owing to flavour-neutral exchange particles, such as gluons or Pomerons [6]. The spin density matrix can be used to examine the exchange process more closely. The first matrix element  $\rho_{00}$  contains all information for an unpolarised beam and target [7]. It can be retrieved entirely from angular distributions where the angle is defined between the normal of the vector meson decay plane and a defined quantisation axis [8]. Furthermore, a differential analysis in  $x_F = 2P_L/\sqrt{s}$ , where  $P_L$  is the longitudinal momentum of the studied particle, allows for a deeper investigation on the interplay of different production mechanisms.

The COMPASS spectrometer set-up [9] meets the need for this kind of measurements due to the large angular acceptance and high momentum resolution. COMPASS is a two-stage fixed-target magnetic spectrometer at the CERN SPS. The analysis outlined in this paper is based on the 2008 and 2009 data taking with 190 GeV hadron beams on a liquid hydrogen target. The positive charged hadron beam consists mainly (75%) of secondary protons which are tagged with a high purity by CEDARs (differential Cherenkov detectors). Pions, protons and kaons in the final state are identified with a RICH detector in the first stage and electromagnetic (ECAL) and hadronic calorimeters in both stages of the set-up. The trigger system selects interactions in the target material by the only requirement of a recoiling proton measured in a cylindrical time-of-flight detector surrounding the target (RPD) which results in a minimum bias on the forward kinematics. Since the  $\omega$  and  $\phi$  mesons are measured simultaneously with the same set-up and the same triggers, systematic uncertainties cancel to large extend.

<sup>a</sup> e-mail: johannes.bernhard@cern.ch

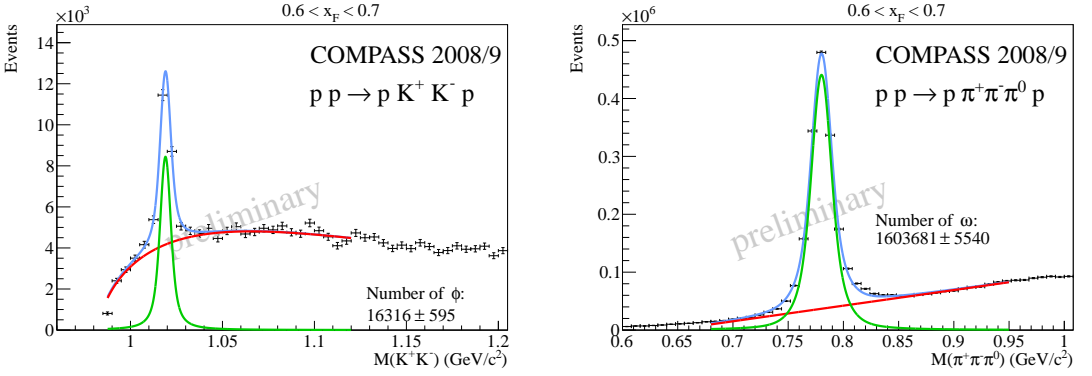


**Fig. 1.** Left: Mass spectrum  $K^+K^-$  with fit to  $\phi(1020)$  signal. Right: Mass spectrum  $\pi^+\pi^-\pi^0$  with fit to  $\omega(782)$  signal. Both spectra are shown exemplarily in the  $0.6 < x_F < 0.7$  range.

## 2 Analysis - OZI Rule

The two channels  $pp \rightarrow p_{fast} \omega p_{recoil}, \omega \rightarrow \pi^+ \pi^- \pi^0$  and  $pp \rightarrow p_{fast} \phi p_{recoil}, \phi \rightarrow K^+ K^-$  are compared to extract  $R(\phi/\omega)$ . In both cases, events were selected with one identified beam proton, one recoil proton in the RPD and three outgoing charged tracks from the primary vertex. The  $\pi^0$  for the  $\omega$  channel was reconstructed from two photons in the ECALs. Additionally, a positive RICH identification of the  $\pi^+$  was required. In the  $\phi$  case, the RICH was used to identify the  $K^+$ . Only exclusive events, *i.e.* events with entirely known kinematics, were selected by requiring the total energy of the final state to match the incident beam energy of 190 GeV and requiring the recoil proton in opposite transverse direction to the forward system<sup>1</sup>. The data were divided into three  $x_F$  bins from 0.6 to 0.9, where  $x_F$  refers to the forward final-state proton  $p_{fast}$ . A multi-dimensional Monte-Carlo based acceptance correction was carried out in the variables  $x_F$ , the four-momentum transfer  $t'$  and  $M(pV)$ , the mass of the vector meson / fast proton - system. Each entry of the relevant  $K^+K^-$  and  $\pi^+\pi^-\pi^0$  mass distributions was corrected for acceptance by application of weights corresponding to the MC acceptance. The yields of  $\phi$  mesons were determined from a Breit-Wigner fit, convoluted with a Gaussian on top of a polynomial background which takes into account the near  $KK$  threshold. The yields of  $\omega$  mesons were determined from a Breit-Wigner fit, convoluted with two Gaussians on top of a polynomial background to take into account the different photon energy resolutions for the two ECALs. Fig. 1 shows exemplary the mass spectra and the corresponding signal extraction in the  $0.6 < x_F < 0.7$  bin. After taking into account the branching in the two studied channels, the preliminary COMPASS data show a violation of the OZI rule prediction with a factor of 3 (*cf.* Tab. 1.a). In Ref. [12] the SPHINX collaboration argued that the OZI rule may not be valid in case of a dominant resonance production part of the cross section. Analogue to Ref. [12], the momentum of the vector meson in the  $pV$  centre-of-mass frame was required to be larger than 1 GeV/c to exclude the mass region which show obvious resonant structures in the  $\omega$  case. In agreement with SPHINX, we observe an increase of the degree of OZI violation to a factor of 6 (*cf.* Tab. 1.b).

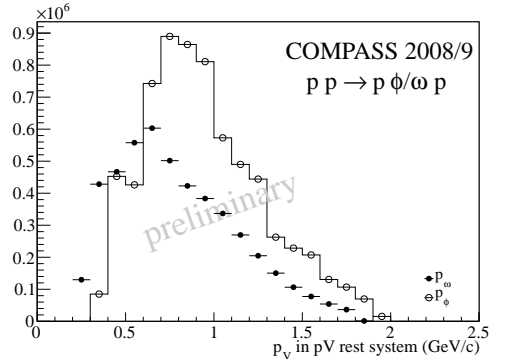


**Fig. 2.** Momentum distribution of  $\phi$  and  $\omega$  mesons in the  $pV$  centre-of-mass frame. The  $\phi$  distribution is scaled with a factor 100 for better illustration.

<sup>1</sup> Further details on selection criteria and kinematic distributions may be found in Ref. [10] and [11].

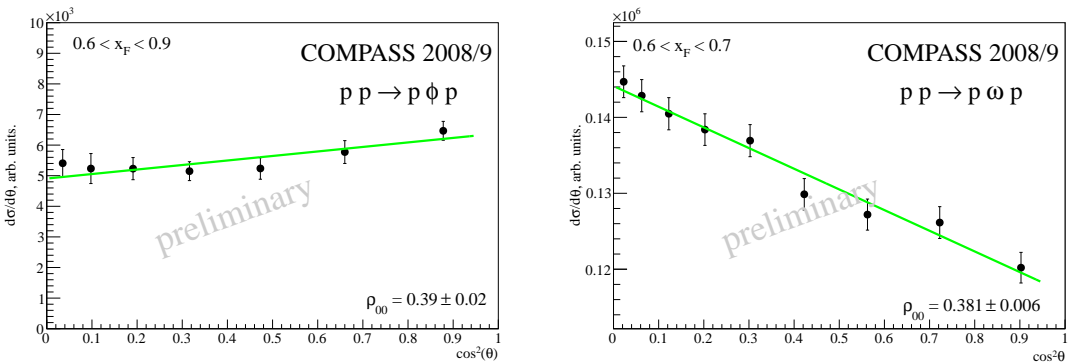
**Table 1.** Ratio of production cross sections  $R(\phi/\omega)$  and errors for different  $x_F$  regions (preliminary).

(a) No $p_V$ cut.					(b) $p_V > 1\text{GeV}/c$ .				
$x_F$	$R(\phi/\omega)$	Stat.	Fit	syst.	$x_F$	$R(\phi/\omega)$	Stat.	Fit	syst.
0.6-0.7	0.019	0.0003	0.0006	0.0037	0.6-0.7	0.032	0.0007	0.0013	0.007
0.7-0.8	0.017	0.0002	0.0004	0.0034	0.7-0.8	0.038	0.0006	0.001	0.007
0.8-0.9	0.012	0.0002	0.0005	0.0024	0.8-0.9	0.019	0.0003	0.0005	0.005

### 3 Analysis - Spin alignment

The analysis is performed in the helicity frame. The helicity angle  $\theta$  is defined in the rest system of the vector meson. The z axis is chosen to be parallel to the direction of the  $p_{fast}V$  system. In the case of the  $\omega$ , we choose the cross product of the two charged pions as an analyser and in the  $\phi$  case the direction of either the  $K^+$  or  $K^-$  is used (*cf.* Ref. [13]) which is chosen randomly. The cross section with a three particle  $\omega$  decay in this choice of  $\theta$  can be parametrised [13] as  $W_{3body}(\cos\theta) = N(2\rho_{00} - (3\rho_{00} - 1)\cos^2\theta)$  (1) and for the  $\phi$  two-body decay as  $W_{2body}(\cos\theta) = N(1 - \rho_{00} + (3\rho_{00} - 1)\cos^2\theta)$  (2). The data are divided in 10 ( $\omega$ ) and 8 ( $\phi$ ) equidistant bins of  $|\cos(\theta)|$  where for the  $\phi$  measurement the closest bin to 0 was removed due to large fit uncertainties. The yields of  $\phi$  and  $\omega$  are retrieved in the same way as described in Sec. 2 and displayed as a function of  $|\cos(\theta)|^2$  to illustrate the linear behaviour in eq. (1) and (2). For  $\phi$ , the data is presented in the region  $0.6 < x_F < 0.9$ . A linear fit is consistent with a small positive slope (Fig. 3, left), *i.e.* no polarisation is observed. Due the better statistics and wider acceptance in  $x_F$  for  $\omega$ , the data is presented in four bins from  $0.2 < x_F < 0.9$ . As an example, Fig. 3, right panel, shows the region  $0.6 < x_F < 0.7$ . Interestingly, we find a clear dependence of  $\rho_{00}$  on  $x_F$  of the final state proton, changing from longitudinal to transverse alignment. The preliminary results for different  $x_F$  regions are summarised in Table 2.

Few comparisons of  $\rho_{00}$  for  $\omega$  and  $\phi$  exist so far, except for photo-production measurements [14]. In hadro-production, only measurements near the threshold are published. For  $\phi$ , the MOMO collaboration finds a complete polarisation in  $pd \rightarrow {}^3\text{He} \phi$  and no polarisation of the  $\omega$  [15]. The WASA collaboration [16] measures within the same reaction the  $\omega$  to be produced unpolarised. The COMPASS data indicate that this behaviour changes with higher beam energies, also largely depending on  $x_F$ .


**Fig. 3.** Differential cross section  $d\sigma/d|\cos\theta|^2$  and linear fit to determine  $\rho_{00}$ . Left:  $\phi$  data in the region  $0.6 < x_F < 0.9$ . Right:  $\omega$  in the region  $0.6 < x_F < 0.7$ .

### Acknowledgements

This work is supported by the German Federal Ministry of Education and Research (BMBF).

**Table 2.** The first spin density matrix element  $\rho_{00}$ , extracted from the helicity angle distributions, and errors for  $\phi$  and  $\omega$  production (preliminary).

Reaction	$x_F$	$\rho_{00}$	Stat.	Fit
$pp \rightarrow pp\phi, \phi \rightarrow K^+ K^-$	0.6-0.9	0.394	0.008	0.018
$pp \rightarrow pp\omega, \omega \rightarrow \pi^+ \pi^- \pi^0$	0.6-0.9	0.306	0.001	0.002
$pp \rightarrow pp\omega, \omega \rightarrow \pi^+ \pi^- \pi^0$	0.2-0.6	0.452	0.002	0.004
$pp \rightarrow pp\omega, \omega \rightarrow \pi^+ \pi^- \pi^0$	0.6-0.7	0.381	0.003	0.005
$pp \rightarrow pp\omega, \omega \rightarrow \pi^+ \pi^- \pi^0$	0.7-0.8	0.337	0.002	0.003
$pp \rightarrow pp\omega, \omega \rightarrow \pi^+ \pi^- \pi^0$	0.8-0.9	0.235	0.001	0.002

## References

1. S. Okubo, Phys. Lett. **5** (1963) 165; G. Zweig, CERN report **TH-401** (1964); J. Iizuka, Prog. Theor. Suppl. **38** (1966) 21.
2. H.J. Lipkin, Phys. Lett. **B 60** (1976) 371.
3. V.P. Nomokonov and M.G. Sapozhnikov, Particles and Nuclei **24** (2003) 184 and references therein.
4. A. Sibirtsev and W. Cassing, Eur. Phys. J. A **7** (2000) 407 and references therein.
5. J. Ellis *et al.*, Phys. Lett. **B 353** (1995) 319;  
J. Ellis *et al.*, Nucl. Phys. A **673** (2000) 256.
6. S.J. Lindenbaum, Nuovo Cim. **65 A** (1981) 222.
7. K. Gottfried and J.D. Jackson, Nuovo Cim. **33** (1964) 302.
8. K. Schilling, P. Seyboth and G. Wolf, Nucl. Phys. B **15** (1970) 397.
9. The COMPASS collaboration, P. Abbon *et al.*, Nucl. Instr. and Meth. A **577** (2007) 455–518;  
The COMPASS collaboration, C. Adolph *et al.*, in preparation for Nucl. Instr. and Meth. A.
10. J. Bernhard and K. Schönning, in *Proceedings of the XIV International Conference on Hadron Spectroscopy (hadron2011)*, Munich, 2011, edited by B. Grube, S. Paul, and N. Brambilla, eConf C110613 (2011) [arXiv:1109.0219]
11. J. Bernhard and K. Schönning, to appear in *Proceedings of Rutherford Centennial Conference on Nuclear Physics*, J. Phys.: Conf. Ser. (2012).
12. S.V. Golovkin *et al.*, Z. Phys. A **359** (1997) 435.
13. The COSY-TOF Collaboration, M. Abdel-Bary *et al.*, Eur. Phys. J. A **44** (2010) 7–22 and references therein.
14. J. Barth *et al.*, Eur. Phys. J A **18** (2003) 117.
15. F. Belleman *et al.*, Phys. Rev. C **75** (2007) 015204.
16. K. Schönning *et al.*, Phys. Lett. B **668** (2008) 258.